Inclusive J, ψ' and $\chi_{\rm c}$ Production in Hadronic Z Decays

L3 Collaboration

Abstract

We report on measurements of the inclusive production of J, ψ' and $\chi_{\rm c}$ mesons in hadronic Z decays, based on 3.2 million hadronic events collected using the L3 detector at LEP. The J and ψ' mesons are reconstructed through their decays into lepton pairs, while the $\chi_{\rm c}$ mesons are reconstructed via the decay mode $\chi_{\rm c} \to {\rm J} + \gamma$. The measured branching fractions are:

$$\begin{aligned}
{\rm Br(Z \to J + X)} &= (3.40 \pm 0.23\,({\rm stat.}) \pm 0.27\,({\rm sys.})) \times 10^{-3} \\
{\rm Br(Z \to \psi' + X)} &= (1.6 \pm 0.5\,({\rm stat.}) \pm 0.3\,({\rm sys.})) \times 10^{-3} \\
{\rm Br(Z \to \chi_{c1} + X)} &= (2.7 \pm 0.6\,({\rm stat.}) \pm 0.5\,({\rm sys.})) \times 10^{-3}.
\end{aligned}$$

In the absence of a clear $\chi_{\rm c2}$ signal, the upper limit at 90% C.L. is set:

$$ {\rm Br(Z \to \chi_{c2} + X)} < 3.2 \times 10^{-3}. $$

Introduction

The production of J, ψ' and χ_c charmonium states in Z decays is predicted to proceed mainly via the decay of b hadrons. Only a minor fraction is expected to be prompt, deriving from the fragmentation of a gluon or a c quark in Z $\to q\overline{q}$ decays. The calculation of Br(b $\to$ J + X) suffers from large QCD uncertainties; the results range from 0.2% to 2% [1–3]. Estimates for the rate of prompt J production Br(Z $\to$ J + X)$_p$ vary from 1×10^{-4} to 4×10^{-4} [4–7].

The interest on quarkonium production has been recently renewed by measurements at the TEVATRON collider [8], which give prompt quarkonium cross sections much higher than predicted by first order color singlet model [9] calculations. It has been shown [10] that the color octet model [11,12] is able to reproduce both the rate and the observed p_t spectrum of $c\overline{c}$ bound states. At LEP present measurements of prompt J production are consistent with both the color octet and the color singlet predictions [13–15]. Features distinctive of the color octet model could show up in the decays of b hadrons into χ_c states, where both color-singlet and color-octet matrix elements contribute at first order [11]. The production of χ_{c1} states could be significantly enhanced, as would be revealed by the value of: $R^b_{\chi_{c1}} = $ Br(b $\to \chi_{c1}$ + X)/Br(b $\to$ J + X), where most of QCD uncertainties cancel out, which in the color singlet model is computed to be $R^b_{\chi_{c1}} \simeq 0.2$ [1]. The production of χ_{c0} and χ_{c2} states, which is strongly suppressed in the color singlet model framework [1], would proceed at first order through the color-octet matrix elements. Since the χ_{c2} has a non-negligible branching fraction into Jγ, its production could result in a visible signal close to the χ_{c1} peak. Moreover, the observation of a large χ_{c2} signal would validate another model of charmonium production, the color evaporation model [16].

We have previously measured the inclusive J and χ_c production in Z decays [13, 17]. The present analysis is performed on the data collected by the L3 experiment [18] from 1991 through 1994, corresponding to 3.2 million hadronic Z decays, with a tripled statistics compared to the previous measurements. An improved resolution for both the J and the χ_c signal is obtained by adopting tighter lepton selection criteria. A direct measurement of the χ_c to J production ratio is performed and the contribution of χ_{c2} states to the signal is investigated.

The branching fractions Br(Z $\to$ J + X) and Br(Z $\to$ ψ' + X)

Hadronic Z decays are selected requiring high multiplicity and high and well balanced visible energy [19]. The selection efficiency is $(98.9 \pm 0.1)\%$, as determined using Z $\to q\overline{q}$ Monte Carlo events [20].

J and ψ' candidates are reconstructed via their decays into muon or electron pairs. Muons are identified and measured in the muon chamber system. Muon tracks are required to consist of track segments in at least two of the three layers of the muon chambers, and to point to the interaction region. Electrons are identified as electromagnetic clusters in the electromagnetic calorimeter associated to a track in the central tracking chamber. Both the barrel and the end cap regions of the calorimeter are used. Tight requirements are made on the shape of the electromagnetic shower and on the quality of the angular and momentum matching with the track. The energy of the electrons is measured using the electromagnetic calorimeter.

In the laboratory system, the J $\to \ell^+\ell^-$ decay typically results in one high and one low momentum lepton. We therefore select muon (electron) candidates with a momentum in excess

---

[1] as can be derived from [1] after accounting for the feed-down from χ_c and ψ' decays into J.

of 2.5 (1.5) GeV for the least energetic one and larger than 4 GeV for the most energetic one. In order to reduce the combinatorial background, we require the opening angle between two oppositely charged lepton candidates to be smaller than $80°$.

Further details on the adopted selection criteria can be found in [21, 22]. All data distributions are in good agreement with the Monte Carlo simulation of 6 million $Z \to q\bar{q}$ decays. In Figure 1 the lepton spectra in the J invariant mass region are shown.

The invariant mass spectra of the selected $\mu^+\mu^-$ and e^+e^- pairs are shown in Figure 2. We perform an unbinned maximum-likelihood fit to the two distributions in the mass region $2.0 < M_{\ell^+\ell^-} < 4.5$ GeV. In this fit the $J \to \ell^+\ell^-$ and $\psi' \to \ell^+\ell^-$ decays are described by two Gaussian functions and the background is modelled using a fourth order polynomial. The two Gaussian functions are constrained to have the same width and a shift of 589 MeV between the central values, corresponding to the known difference between the ψ' and J masses [23]. From the fit we obtain 241 ± 25 $J \to \mu^+\mu^-$ and 200 ± 18 $J \to e^+e^-$ decays, together with 27 ± 10 $\psi' \to \mu^+\mu^-$ and 12 ± 7 $\psi' \to e^+e^-$ candidates. The resulting mass values and resolutions for the J signal are: $M_J^{\mu^+\mu^-} = (3118 \pm 12)$ MeV, $\sigma_{\mu^+\mu^-} = (123 \pm 12)$ MeV and $M_J^{e^+e^-} = (3093 \pm 8)$ MeV, $\sigma_{e^+e^-} = (85 \pm 9)$ MeV, in agreement with the expectations from the Monte Carlo simulation.

The signal is simulated by 16000 Monte Carlo $Z \to b\bar{b}$ events [20], imposing the decay chain $b \to J + X$ followed by $J \to \ell^+\ell^-$ for one of the b hadrons. The Peterson fragmentation function for b quarks is used with $< x_b >= 0.702$ in accordance with the LEP measurements [24]. The generated events are reweighted according to the J momentum in the B reference system, in order to reproduce measurements performed at the $\Upsilon(4S)$ [25]. From the Monte Carlo simulation we estimate the selection efficiencies $\epsilon_J^{\mu^+\mu^-} = 0.259 \pm 0.005$ and $\epsilon_J^{e^+e^-} = 0.212 \pm 0.005$, where the quoted errors are statistical only.

The summary of the relative systematic errors on $Br(Z \to J + X)$ is given in Table 1. Uncertainties due to the adopted lepton identification criteria are evaluated by varying the lepton identification parameters. The cut on the least energetic lepton momentum is varied in the $(2-4)$ GeV range for muons and $(1-3)$ GeV range for electrons; the cut on the most energetic lepton momentum is varied in the $(2-6)$ GeV range. We also vary the angular cut between the two leptons, in the $60° - 100°$ range. The total variation on $Br(Z \to J + X)$ observed by varying kinematical cuts is 3.9%, to be compared to the 2% uncertainty estimated by varying $< x_b >$ between 0.711 and 0.695 in the Monte Carlo simulation of the signal. Detector inefficiencies are evaluated using the online database information, and checked with an alternative method, based on the analysis of $Z \to \ell^+\ell^-$ decays. Relative to a fully efficient detector, acceptance factors of 0.81 ± 0.06 for $J \to e^+e^-$ and 0.85 ± 0.05 for $J \to \mu^+\mu^-$ decays are estimated, where the quoted errors are conservatively derived from the difference of the two evaluations. The fitting procedure is checked by counting the number of events inside the invariant mass window $M_J \pm 3\sigma_{\ell^+\ell^-}$ and subtracting the background found in simulated $Z \to q\bar{q}$ decays. Using $Br(J \to \ell^+\ell^-) = 0.0601 \pm 0.0019$ [23], we measure:

$$
\begin{aligned}
Br(Z \to J(e^+e^-) + X) &= (3.42 \pm 0.31 \pm 0.35) \times 10^{-3}; \\
Br(Z \to J(\mu^+\mu^-) + X) &= (3.38 \pm 0.35 \pm 0.32) \times 10^{-3}.
\end{aligned}
$$

Combining the two measurements and taking into account common systematic errors, we obtain the following branching fraction:

$$
Br(Z \to J + X) = (3.40 \pm 0.23 \pm 0.27) \times 10^{-3}.
$$

	$\Delta\mathrm{Br}(Z \to J + X)/\mathrm{Br}(Z \to J + X)$		
	$J \to e^+e^-$	$J \to \mu^+\mu^-$	$J \to \ell^+\ell^-$
Lepton identification	3.5 %	2.2 %	2.2 %
Kinematical cuts	3.7 %	4.1 %	3.9 %
Detector inefficiencies	7.4 %	6.2 %	5.0 %
M.C. statistics	1.8 %	1.8 %	1.3 %
Fitting procedure	3.5 %	3.9 %	2.6 %
$\mathrm{Br}(J \to \ell^+\ell^-)$	3.2 %	3.2 %	3.2 %
Total	10.1 %	9.4 %	7.9 %

Table 1: Relative systematic errors on the measurement of Br(Z →J+ X). The contributions from $J \to e^+ e^-$, $J \to \mu^+ \mu^-$ and the combined channel are detailed.

From the number of reconstructed $\psi' \to \ell^+\ell^-$ decays we measure:

$$\mathrm{Br}(Z \to \psi' + X) = (1.6 \pm 0.5 \pm 0.3) \times 10^{-3}$$

where the major systematic uncertainty arises from the evaluation of the background under the ψ' peak and from the knowledge of $\mathrm{Br}(\psi' \to \ell^+\ell^-)$ [23].

The branching fractions $\mathrm{Br}(b \to J + X)$ and $\mathrm{Br}(b \to \psi' + X)$ can be evaluated, taking into account the fraction of J and ψ' not produced in b decays. The estimates of prompt J production yield values of $\mathrm{Br}(Z \to J + X)_{\mathrm{p}}$ from 1×10^{-4} to 4×10^{-4}, depending on the model adopted and with at least a factor two uncertainty in the calculations [4–7]. Present experimental results on prompt J production [13–15] are consistent with these predictions. We therefore use: $\mathrm{Br}(Z \to J + X)_{\mathrm{p}} = (2 \pm 2) \times 10^{-4}$. For prompt ψ' production we use $\mathrm{Br}(Z \to \psi' + X)_{\mathrm{p}} = (1 \pm 1) \times 10^{-4}$ [7]. Assuming the Standard Model value $R_{\mathrm{b}} = 0.2156$ [26], we derive:

$$\mathrm{Br}(b \to J + X) = (1.06 \pm 0.08 \pm 0.11) \times 10^{-2}$$
$$\mathrm{Br}(b \to \psi' + X) = (0.46 \pm 0.16 \pm 0.08) \times 10^{-2}.$$

The branching fraction $\mathrm{Br}(Z \to \chi_{c1} + X)$

Inclusive χ_{c1} meson production in Z decays is measured via the $\chi_{c1} \to J\gamma$ decay. In order to increase the statistics in the $J \to e^+ e^-$ channel, some of the electromagnetic identification criteria are relaxed. A total number of 440 ± 32 (background subtracted) $J \to \ell^+\ell^-$ events are selected in the mass window between 2.8 and 3.4 GeV.

Photon candidates are identified as isolated clusters in the electromagnetic calorimeter having a shape consistent with an electromagnetic shower, and with no charged track pointing to the cluster within four times the expected angular resolution in the azimuthal plane. In order to reduce the combinatorial background, only photons inside a 40° cone around the reconstructed J direction and with energy larger than 1.1 GeV are selected. Further details on the selection variables can be found in [22].

The χ_{c1} candidates are selected in the $M(\ell^+\ell^-\gamma) - M(\ell^+\ell^-) = (414 \pm 56)$ MeV mass-difference window, which is centred around the $M(\chi_{c1}) - M(J)$ expected value [23], and about three times wider than the average Monte Carlo resolution, $\sigma_{\mathrm{MC}} = 18.7$ MeV. Figure 3 shows

the energy spectrum of photons selected in the signal mass region and Figure 4 the momentum of the selected χ_{c1} candidates. In Figure 5 the measured $M(\ell^+\ell^-\gamma) - M(\ell^+\ell^-)$ spectrum is shown. A total of 64 events is selected in the chosen signal region.

The background can be divided in two components: events where a fake J is selected and events where a true J is combined with an uncorrelated photon. The background due to fake J is studied using data taken from the sidebands of the J peak and from $e^\pm\mu^\mp$ pairs in the J mass region. The background due to random $J - \gamma$ combinations is studied through $Z \to J + X$ Monte Carlo events, excluding χ_c production. The obtained distributions are shown in Figure 6. Their shapes are similar, and no residual structure is seen in $J - \gamma$ combinations. The total expected background shape is obtained by summing the two contributions, weighted according to the signal to background ratio found under the J mass peak. A function of the form: $f_{BG}(x) = A \cdot \exp(a\,x + b/x^2)$, where $x = M(\ell^+\ell^-\gamma) - M(\ell^+\ell^-)$, is used to describe the background shape. The a and b parameters are determined through a maximum-likelihood fit. The normalisation factor A is derived from the data events counted in the side bands of the χ_c mass window. After background subtraction, the number of observed χ_{c1} candidates is $N(\chi_{c1}) = 32.8 \pm 8.0$.

The χ_{c1} signal is simulated using $Z \to b\overline{b}$ decays [20]. The acceptance for finding the χ_{c1}, once the J has been selected, is 0.342 ± 0.007. The total efficiency, including the J selection, is found to be 0.081 ± 0.004, where the errors are statistical.

The evaluation of systematic uncertainties on both the $\text{Br}(Z \to \chi_{c1} + X)$ and $R^Z_{\chi_{c1}} = \text{Br}(Z \to \chi_{c1} + X)/\text{Br}(Z \to J + X)$ measurements is summarised in Table 2. We vary the cut on the energy of the photon between 0.5 and 1.5 GeV. The acceptance angle between the photon and the J direction is varied between $20°$ and $60°$. Varying also the shower shape and isolation requirements, we estimate the total systematic error induced by the photon selection to be 10%. The systematic errors induced by the J selection efficiency cancel out in the $R^Z_{\chi_{c1}}$ ratio. This ratio is however affected by the purity of J selected in the dilepton sample.

The determination of the a, b parameters and of the normalisation of the function f_{BG} gives a statistical error on the background under the χ_{c1} signal region of 7.4%. We assume that all the selected candidates are from χ_{c1} decays. We do not expect any contamination due to χ_{c0} mesons, since their branching fraction into $J\,\gamma$ is negligible. The contamination due to $\chi_{c2} \to J\,\gamma$ decays has, however, to be investigated. A χ_{c2} signal would be located at $M(\ell^+\ell^-\gamma) - M(\ell^+\ell^-) = 459.29$ MeV. Shrinking the width of the acceptance window around the expected χ_{c1} signal position by σ_{MC}, we obtain a 7% increase of the measured branching fraction; enlarging the acceptance window by σ_{MC} results in a 3% decrease. As a further check, an alternative counting procedure is adopted. We perform an unbinned maximum-likelihood fit to the $M(\ell^+\ell^-\gamma) - M(\ell^+\ell^-)$ distribution. The same function $f_{BG}(x)$ is used to describe the background, but a and b are left as free parameters in the fit. Two Gaussian shapes are used for the χ_{c1} and the χ_{c2} signal, constrained to have the same width and a shift between central values consistent with the known $M_{\chi_{c2}} - M_{\chi_{c1}}$ mass difference of 45.6 MeV [23]. The result of this fit is shown in Figure 7. We obtain a mass difference $M(\chi_{c1}) - M(J)$ of $413.2^{+3.6}_{-3.0}$ MeV, consistent with the expected value of 413.65 ± 0.13 MeV [23]. The fitted resolution is $10.8^{+3.5}_{-2.5}$ MeV. The numbers of χ_{c1} and χ_{c2} candidates found by the fit are $N^{fit}_{\chi_{c1}} = 30.1^{+7.7}_{-7.0}$ and $N^{fit}_{\chi_{c2}} = 8.8^{+5.4}_{-4.6}$. $N^{fit}_{\chi_{c1}}$ is in good agreement with the $N(\chi_{c1})$ value obtained previously in this paper. Including the variation of $\text{Br}(Z \to \chi_{c1} + X)$ observed by changing the mass-difference acceptance window, we assign to the counting procedure a relative systematic error of $\pm 8\%$.

Using $\text{Br}(\chi_{c1} \to J\,\gamma) = 0.273 \pm 0.016$ [23] we derive:

$$\text{Br}(Z \to \chi_{c1} + X) = (2.7 \pm 0.6 \pm 0.5) \times 10^{-3}$$

	$\Delta R^{\mathrm{Z}}_{\chi_{c1}}/R^{\mathrm{Z}}_{\chi_{c1}}$	$\Delta\mathrm{Br}/\mathrm{Br}_{(\mathrm{Z}\to\chi_{c1}+\mathrm{X})}$
M.C. statistics	2 %	5 %
γ selection	10 %	10 %
J purity	4 %	–
$\Delta\epsilon_{\mathrm{J}}/\epsilon_{\mathrm{J}}$	–	7 %
Bkg. subtraction	7 %	7 %
χ_c counting	8 %	8 %
$\Delta\mathrm{Br}/\mathrm{Br}_{(\chi_{c1}\to\mathrm{J}+\gamma)}$	6 %	6 %
$\Delta\mathrm{Br}/\mathrm{Br}_{(\mathrm{J}\to\ell^{+}\ell^{-})}$	–	3 %
Total	17 %	18 %

Table 2: Relative systematic errors on the measurement of $R^{\mathrm{Z}}_{\chi_{c1}}$ and $\mathrm{Br}(\mathrm{Z}\to\chi_{c1}+\mathrm{X})$.

$$R^{\mathrm{Z}}_{\chi_{c1}} = 0.80 \pm 0.19 \pm 0.14$$

Using the results from the two-Gaussian fit, the 90% confidence level of the likelihood function corresponds to an upper limit of 16 observed χ_{c2} events. Using $\mathrm{Br}(\chi_{c2}\to\mathrm{J}\,\gamma)=0.135\pm0.011$ [23] and accounting for systematic errors, we set an upper limit:

$$\mathrm{Br}(\mathrm{Z}\to\chi_{c2}+\mathrm{X}) < 3.2 \times 10^{-3}$$

at the 90% confidence level.

The χ_{c1} production rate from fragmentation processes is expected to be of the same order of magnitude as the J. The color singlet prediction is $\mathrm{Br}(\mathrm{Z}\to\chi_{c1}+\mathrm{X})_{\mathrm{p}}\simeq0.5\times10^{-4}$ [4] whereas a higher value, around 1.4×10^{-4}, is expected in the color octet framework [7]. Assuming $\mathrm{Br}(\mathrm{Z}\to\chi_{c1}+\mathrm{X})_{\mathrm{p}}=(1.4\pm1.4)\times10^{-4}$ we derive:

$$\mathrm{Br}(\mathrm{b}\to\chi_{c1}+\mathrm{X}) = (0.84\pm0.20\pm0.16)\times10^{-2}.$$

Even assuming prompt χ_{c1} production but no prompt J production, our $R^{\mathrm{Z}}_{\chi_{c1}}$ measurement corresponds to: $R^{\mathrm{b}}_{\chi_{c1}}=0.75\pm0.19\pm0.15$, which is significantly higher than the color singlet model expectation $R^{\mathrm{b}}_{\chi_{c1}}\simeq0.2$.

Summary

With a sample of 3.2 million hadronic Z decays we obtain:

$$\begin{aligned}
\mathrm{Br}(\mathrm{Z}\to\mathrm{J}+\mathrm{X}) &= (3.40\pm0.23\,(\mathrm{stat.})\pm0.27\,(\mathrm{sys.}))\times10^{-3} \\
\mathrm{Br}(\mathrm{Z}\to\psi'+\mathrm{X}) &= (1.6\pm0.5\,(\mathrm{stat.})\pm0.3\,(\mathrm{sys.}))\times10^{-3} \\
\mathrm{Br}(\mathrm{Z}\to\chi_{c1}+\mathrm{X}) &= (2.7\pm0.6\,(\mathrm{stat.})\pm0.5\,(\mathrm{sys.}))\times10^{-3}.
\end{aligned}$$

These results improve and supersede our previous measurements [13,17]. The results on J and ψ' are consistent with the other LEP measurements [14, 27]. The result on χ_{c1} is the most accurate today.

We obtain a 90% C.L. upper limit:

$$\mathrm{Br}(\mathrm{Z}\to\chi_{c2}+\mathrm{X}) < 3.2\times10^{-3}.$$

If assumptions on the contribution to charmonium production due to fragmentation processes are made, the measured inclusive Z decay rates can be related to b decays. While the inferred $b \to J (\psi', \chi_{c1}) + X$ rates are consistent with measurements performed at the $\Upsilon(4S)$ [25, 28], the $Br(b \to \chi_{c1} + X)/Br(b \to J + X)$ ratio is higher than expected from first-order color singlet model calculations, and suggests the existence of additional mechanisms of quarkonia production.

Acknowledgements

References

[1] J.H. Kühn, S. Nussinov, R. Rückl, Z. Phys. **C 5** (1980) 117;
J.H. Kühn, R. Rückl, Phys. Lett. **B 135** (1984) 477.

[2] L. Bergström, P. Ernström, Phys. Lett. **B 328** (1994) 153.

[3] P. Ko, J. Lee, H.S. Song, Phys. Rev. **D 53** (1996) 1409; ibid **D 54** (1996) 4312.

[4] K. Hagiwara, A.D. Martin, W.J. Stirling, Phys. Lett. **B267** (1991) 527; *erratum*: ibid **B316** (1993) 635).

[5] V. Barger, K. Cheung, W.Y. Keung, Phys. Rev. **D 41** (1991) 1541;
E. Braaten, K. Cheung, Phys. Rev. **D 48** (1993) 4230.

[6] K. Cheung, W.Y. Keung, T.C. Yuan, Phys. Rev. Lett. **76** (1996) 877;
P. Cho, Phys. Lett. **B 368** (1996) 171;
S. Baek, P. Ko, J. Lee, H.S. Song, Phys. Lett. **B 389** (1996) 609.

[7] G.A. Schuler, CERN-TH/97-12 (hep-ph/9702230).

[8] CDF Collaboration, F. Abe *et al.*, Phys. Rev. Lett. **69** (1992) 3704;
CDF Collaboration, F. Abe *et al.* Fermilab-PUB-97/024E.

[9] E.L. Berger, D. Jones, Phys. Rev. **D 23** (1981) 1521;
E.L. Berger, D. Jones, Phys. Lett. **B 121** (1983) 61;
R. Baier, R. Rückl, Z. Phys. **C 19** (1983) 251.

[10] M. Cacciari, M. Greco, M.L. Mangano, A. Petrelli, Phys. Lett. **B 356** (1995) 553;
E. Braaten, S. Fleming, Phys. Rev. Lett. **74** (1995) 3327;
P. Cho, M. Wise, Phys. Lett. **B 346** (1995) 129.

[11] G.T. Bodwin, E. Braaten, T.C. Yuan, G.P. Lepage, Phys. Rev. **D 46** (1992) 3703.

[12] G.T. Bodwin, E. Braaten, G.P. Lepage, Phys. Rev. **D 51** (1995) 1125;
E. Braaten, S. Fleming, T.C. Yuan, Ann. Rev. Nucl. Part. Sci. **46** (1996) 197.

[13] L3 Collab., O. Adriani *et al.*, Phys. Lett. **B 288** (1992) 412.

[14] DELPHI Collab., P. Abreu *et al.*, Phys. Lett. **B 341** (1994) 109.

[15] OPAL Collab., G. Alexander *et al.*, Phys. Lett. **B 384** (1996) 343.

[16] See, e.g., G.A. Schuler, Z Phys **C71** (1996),317; CERN-TH.7170/94 (hep-ph/9403387) and references therein.

[17] L3 Collab., O. Adriani *et al.*, Phys. Lett. **B 317** (1993) 467.

[18] L3 Collab., B. Adeva *et al.*, Nucl. Inst. Meth. **A 289** (1990) 35;
L3 Collab., M. Acciarri *et al.*, Nucl. Inst. Meth. **A 351** (1994) 300;
L3 Collab., O. Adriani *et al.*, Physics Reports **236** (1993) 1.

[19] L3 Collab., M. Acciarri *et al.*, Z. Phys. **C 62** (1994) 551.

[20] T. Sjöstrand, Comp. Phys. Comm. **39** (1986) 347;
T. Sjöstrand and M. Bengtsson, Comp. Phys. Comm. **43** (1987) 367;
T.Sjöstrand, Comp. Phys. Comm. **82** (1994) 74.

[21] M. Rattaggi, "Misura della produzione della particella J/ψ nell'esperimento L3 a LEP" Ph.D. thesis, 1995 Università degli Studi di Milano.

[22] S. Paoletti,"Studio della produzione di J/ψ a LEP" Ph.D. thesis, 1996 Università degli Studi di Roma "La Sapienza".

[23] Particle Data Group, Phys. Rev. **D 54** (1996) I.54.

[24] The LEP heavy flavour group, LEPHF/96-01, ALEPH Note 96-099, DELPHI 96-67 PHYS 627, L3 Note 1969, OPAL Technical Note TN391.

[25] CLEO Collab., R. Balest *et al.*, Phys. Rev. **D 52** (1995) 2661.

[26] The LEP Collaborations ALEPH, DELPHI, L3, OPAL and the Electroweak Working Group, CERN-PPE/95-172.

[27] ALEPH Collab., D. Buskulic *et al.*, Phys. Lett. **B 295** (1992) 396;
OPAL Collab., G. Alexander *et al.*, Z. Phys. **C 70** (1996) 197.

[28] ARGUS Collab., H. Albrecht *et al.*, Phys. Lett. **B 277** (1992) 209.

The L3 Collaboration:

M.Acciarri,[28] O.Adriani,[17] M.Aguilar-Benitez,[27] S.Ahlen,[11] J.Alcaraz,[27] G.Alemanni,[23] J.Allaby,[18] A.Aloisio,[30]
G.Alverson,[12] M.G.Alviggi,[30] G.Ambrosi,[20] H.Anderhub,[50] V.P.Andreev,[39] T.Angelescu,[13] F.Anselmo,[9] A.Arefiev,[29]
T.Azemoon,[3] T.Aziz,[10] P.Bagnaia,[38] L.Baksay,[45] R.C.Ball,[3] S.Banerjee,[10] Sw.Banerjee,[10] K.Banicz,[47] A.Barczyk,[50,ψ]
R.Barillère,[18] L.Barone,[38] P.Bartalini,[35] A.Baschirotto,[28] M.Basile,[9] R.Battiston,[35] A.Bay,[23] F.Becattini,[17] U.Becker,[16]
F.Behner,[50] J.Berdugo,[27] P.Berges,[16] B.Bertucci,[35] B.L.Betev,[50] S.Bhattacharya,[10] M.Biasini,[18] A.Biland,[50]
G.M.Bilei,[35] J.J.Blaising,[4] S.C.Blyth,[36] G.J.Bobbink,[2] R.Bock,[1] A.Böhm,[1] L.Boldizsar,[14] B.Borgia,[38] A.Boucham,[4]
D.Bourilkov,[50] M.Bourquin,[20] D.Boutigny,[4] S.Braccini,[20] J.G.Branson,[41] V.Brigljevic,[50] I.C.Brock,[36] A.Buffini,[17]
A.Buijs,[46] J.D.Burger,[16] W.J.Burger,[20] J.Busenitz,[45] X.D.Cai,[16] M.Campanelli,[50] M.Capell,[16] G.Cara Romeo,[9]
G.Carlino,[30] A.M.Cartacci,[17] J.Casaus,[27] G.Castellini,[17] F.Cavallari,[38] N.Cavallo,[30] C.Cecchi,[20] M.Cerrada,[27]
F.Cesaroni,[24] M.Chamizo,[27] Y.H.Chang,[52] U.K.Chaturvedi,[19] S.V.Chekanov,[32] M.Chemarin,[26] A.Chen,[52] G.Chen,[7]
G.M.Chen,[7] H.F.Chen,[21] H.S.Chen,[7] M.Chen,[16] G.Chiefari,[30] C.Y.Chien,[5] L.Cifarelli,[40] F.Cindolo,[9] C.Civinini,[17]
I.Clare,[16] R.Clare,[16] H.O.Cohn,[33] G.Coignet,[4] A.P.Colijn,[2] N.Colino,[27] V.Commichau,[1] S.Costantini,[8] F.Cotorobai,[13]
B.de la Cruz,[27] A.Csilling,[14] T.S.Dai,[16] R.D'Alessandro,[17] R.de Asmundis,[30] A.Degré,[4] K.Deiters,[48] P.Denes,[37]
F.DeNotaristefani,[38] D.DiBitonto,[45] M.Diemoz,[38] D.van Dierendonck,[2] F.Di Lodovico,[50] C.Dionisi,[38] M.Dittmar,[50]
A.Dominguez,[41] A.Doria,[30] I.Dorne,[4] M.T.Dova,[19,♯] E.Drago,[30] D.Duchesneau,[4] P.Duinker,[2] I.Duran,[42] S.Dutta,[10]
S.Easo,[35] Yu.Efremenko,[33] H.El Mamouni,[26] A.Engler,[36] F.J.Eppling,[16] F.C.Erné,[2] J.P.Ernenwein,[26] P.Extermann,[20]
M.Fabre,[48] R.Faccini,[38] S.Falciano,[38] A.Favara,[17] J.Fay,[26] O.Fedin,[39] M.Felcini,[50] B.Fenyi,[45] T.Ferguson,[36] F.Ferroni,[38]
H.Fesefeldt,[1] E.Fiandrini,[35] J.H.Field,[20] F.Filthaut,[36] P.H.Fisher,[16] I.Fisk,[41] G.Forconi,[16] L.Fredj,[20] K.Freudenreich,[50]
C.Furetta,[28] Yu.Galaktionov,[29,16] S.N.Ganguli,[10] P.Garcia-Abia,[49] S.S.Gau,[12] S.Gentile,[38] J.Gerald,[5]
N.Gheordanescu,[13] S.Giagu,[38] S.Goldfarb,[23] J.Goldstein,[11] Z.F.Gong,[21] A.Gougas,[5] G.Gratta,[34] M.W.Gruenewald,[8]
V.K.Gupta,[37] A.Gurtu,[10] L.J.Gutay,[47] B.Hartmann,[1] A.Hasan,[31] D.Hatzifotiadou,[9] T.Hebbeker,[8] A.Hervé,[18]
W.C.van Hoek,[32] H.Hofer,[50] S.J.Hong,[44] H.Hoorani,[36] S.R.Hou,[52] G.Hu,[5] V.Innocente,[18] H.Janssen,[4] K.Jenkes,[1]
B.N.Jin,[7] L.W.Jones,[3] P.de Jong,[18] I.Josa-Mutuberria,[27] A.Kasser,[23] R.A.Khan,[19] D.Kamrad,[49] Yu.Kamyshkov,[33]
J.S.Kapustinsky,[25] Y.Karyotakis,[4] M.Kaur,[19,♢] M.N.Kienzle-Focacci,[20] D.Kim,[38] D.H.Kim,[44] J.K.Kim,[44] S.C.Kim,[44]
Y.G.Kim,[44] W.W.Kinnison,[25] A.Kirkby,[34] D.Kirkby,[34] J.Kirkby,[18] D.Kiss,[14] W.Kittel,[32] A.Klimentov,[16,29]
A.C.König,[32] A.Kopp,[49] I.Korolko,[29] V.Koutsenko,[16,29] R.W.Kraemer,[36] W.Krenz,[1] A.Kunin,[16,29]
P.Ladron de Guevara,[27] G.Landi,[17] C.Lapoint,[16] K.Lassila-Perini,[50] P.Laurikainen,[22] M.Lebeau,[18] A.Lebedev,[16]
P.Lebrun,[26] P.Lecomte,[50] P.Lecoq,[18] P.Le Coultre,[50] C.Leggett,[3] J.M.Le Goff,[18] R.Leiste,[49] E.Leonardi,[38]
P.Levtchenko,[39] C.Li,[21] C.H.Lin,[52] W.T.Lin,[52] F.L.Linde,[2,18] L.Lista,[30] Z.A.Liu,[7] W.Lohmann,[49] E.Longo,[38] W.Lu,[34]
Y.S.Lu,[7] K.Lübelsmeyer,[1] C.Luci,[38] D.Luckey,[16] L.Luminari,[38] W.Lustermann,[48] W.G.Ma,[21] M.Maity,[10]
G.Majumder,[10] L.Malgeri,[38] A.Malinin,[29] C.Maña,[27] D.Mangeol,[32] S.Mangla,[10] P.Marchesini,[50] A.Marin,[11]
J.P.Martin,[26] F.Marzano,[38] G.G.G.Massaro,[2] D.McNally,[18] S.Mele,[30] L.Merola,[30] M.Meschini,[17] W.J.Metzger,[32]
M.von der Mey,[1] Y.Mi,[23] A.Mihul,[13] A.J.W.van Mil,[32] G.Mirabelli,[38] J.Mnich,[18] P.Molnar,[8] B.Monteleoni,[17]
R.Moore,[3] S.Morganti,[38] T.Moulik,[10] R.Mount,[34] S.Müller,[1] F.Muheim,[20] A.J.M.Muijs,[2] S.Nahn,[16] M.Napolitano,[30]
F.Nessi-Tedaldi,[50] H.Newman,[34] T.Niessen,[1] A.Nippe,[1] A.Nisati,[38] H.Nowak,[49] Y.D.Oh,[44] H.Opitz,[1] G.Organtini,[38]
R.Ostonen,[22] C.Palomares,[27] D.Pandoulas,[1] S.Paoletti,[38] P.Paolucci,[30] H.K.Park,[36] I.H.Park,[44] G.Pascale,[38]
G.Passaleva,[17] S.Patricelli,[30] T.Paul,[12] M.Pauluzzi,[35] C.Paus,[1] F.Pauss,[50] D.Peach,[18] Y.J.Pei,[1] S.Pensotti,[28]
D.Perret-Gallix,[4] B.Petersen,[32] S.Petrak,[8] A.Pevsner,[5] D.Piccolo,[30] M.Pieri,[17] J.C.Pinto,[36] P.A.Piroué,[37] E.Pistolesi,[28]
V.Plyaskin,[29] M.Pohl,[50] V.Pojidaev,[29,17] H.Postema,[16] N.Produit,[20] D.Prokofiev,[39] G.Rahal-Callot,[50] N.Raja,[10]
P.G.Rancoita,[28] M.Rattaggi,[28] G.Raven,[41] P.Razis,[31] K.Read,[33] D.Ren,[50] M.Rescigno,[38] S.Reucroft,[12] T.van Rhee,[46]
S.Riemann,[49] K.Riles,[3] O.Rind,[3] A.Robohm,[50] J.Rodin,[16] B.P.Roe,[3] L.Romero,[27] S.Rosier-Lees,[4] Ph.Rosselet,[23]
W.van Rossum,[46] S.Roth,[1] J.A.Rubio,[18] D.Ruschmeier,[8] H.Rykaczewski,[50] J.Salicio,[18] E.Sanchez,[27] M.P.Sanders,[32]
M.E.Sarakinos,[22] S.Sarkar,[10] M.Sassowsky,[1] G.Sauvage,[4] C.Schäfer,[1] V.Schegelsky,[39] S.Schmidt-Kaerst,[1] D.Schmitz,[1]
P.Schmitz,[1] M.Schneegans,[4] N.Scholz,[50] H.Schopper,[51] D.J.Schotanus,[32] J.Schwenke,[1] G.Schwering,[1] C.Sciacca,[30]
D.Sciarrino,[20] L.Servoli,[35] S.Shevchenko,[34] N.Shivarov,[43] V.Shoutko,[29] J.Shukla,[25] E.Shumilov,[29] A.Shvorob,[34]
T.Siedenburg,[1] D.Son,[44] A.Sopczak,[49] V.Soulimov,[30] B.Smith,[16] P.Spillantini,[17] M.Steuer,[16] D.P.Stickland,[37]
H.Stone,[37] B.Stoyanov,[43] A.Straessner,[1] K.Strauch,[15] K.Sudhakar,[10] G.Sultanov,[19] L.Z.Sun,[21] G.F.Susinno,[20]
H.Suter,[50] J.D.Swain,[19] X.W.Tang,[7] L.Tauscher,[6] L.Taylor,[12] Samuel C.C.Ting,[16] S.M.Ting,[16] M.Tonutti,[1]
S.C.Tonwar,[10] J.Tóth,[14] C.Tully,[37] H.Tuchscherer,[45] K.L.Tung,[7] Y.Uchida,[16] J.Ulbricht,[50] U.Uwer,[18] E.Valente,[38]
R.T.Van de Walle,[32] G.Vesztergombi,[14] I.Vetlitsky,[29] G.Viertel,[50] M.Vivargent,[4] R.Völkert,[49] H.Vogel,[36] H.Vogt,[49]
I.Vorobiev,[29] A.A.Vorobyov,[39] A.Vorvolakos,[31] M.Wadhwa,[6] W.Wallraff,[1] J.C.Wang,[16] X.L.Wang,[21] Z.M.Wang,[21]
A.Weber,[1] F.Wittgenstein,[18] S.X.Wu,[19] S.Wynhoff,[1] J.Xu,[11] Z.Z.Xu,[21] B.Z.Yang,[21] C.G.Yang,[7] X.Y.Yao,[7] J.B.Ye,[21]
S.C.Yeh,[52] J.M.You,[36] An.Zalite,[39] Yu.Zalite,[39] P.Zemp,[50] Y.Zeng,[1] Z.Zhang,[7] Z.P.Zhang,[21] B.Zhou,[11] Y.Zhou,[3]
G.Y.Zhu,[7] R.Y.Zhu,[34] A.Zichichi,[9,18,19] F.Ziegler.[49]

1   I. Physikalisches Institut, RWTH, D-52056 Aachen, FRG[§]
    III. Physikalisches Institut, RWTH, D-52056 Aachen, FRG[§]
2   National Institute for High Energy Physics, NIKHEF, and University of Amsterdam, NL-1009 DB Amsterdam,
    The Netherlands
3   University of Michigan, Ann Arbor, MI 48109, USA
4   Laboratoire d'Annecy-le-Vieux de Physique des Particules, LAPP,IN2P3-CNRS, BP 110, F-74941
    Annecy-le-Vieux CEDEX, France
5   Johns Hopkins University, Baltimore, MD 21218, USA
6   Institute of Physics, University of Basel, CH-4056 Basel, Switzerland
7   Institute of High Energy Physics, IHEP, 100039 Beijing, China[△]
8   Humboldt University, D-10099 Berlin, FRG[§]
9   University of Bologna and INFN-Sezione di Bologna, I-40126 Bologna, Italy
10 Tata Institute of Fundamental Research, Bombay 400 005, India
11 Boston University, Boston, MA 02215, USA
12 Northeastern University, Boston, MA 02115, USA
13 Institute of Atomic Physics and University of Bucharest, R-76900 Bucharest, Romania
14 Central Research Institute for Physics of the Hungarian Academy of Sciences, H-1525 Budapest 114, Hungary[‡]
15 Harvard University, Cambridge, MA 02139, USA
16 Massachusetts Institute of Technology, Cambridge, MA 02139, USA
17 INFN Sezione di Firenze and University of Florence, I-50125 Florence, Italy
18 European Laboratory for Particle Physics, CERN, CH-1211 Geneva 23, Switzerland
19 World Laboratory, FBLJA Project, CH-1211 Geneva 23, Switzerland
20 University of Geneva, CH-1211 Geneva 4, Switzerland
21 Chinese University of Science and Technology, USTC, Hefei, Anhui 230 029, China[△]
22 SEFT, Research Institute for High Energy Physics, P.O. Box 9, SF-00014 Helsinki, Finland
23 University of Lausanne, CH-1015 Lausanne, Switzerland
24 INFN-Sezione di Lecce and Universitá Degli Studi di Lecce, I-73100 Lecce, Italy
25 Los Alamos National Laboratory, Los Alamos, NM 87544, USA
26 Institut de Physique Nucléaire de Lyon, IN2P3-CNRS,Université Claude Bernard, F-69622 Villeurbanne, France
27 Centro de Investigaciones Energeticas, Medioambientales y Tecnologicas, CIEMAT, E-28040 Madrid, Spain[♭]
28 INFN-Sezione di Milano, I-20133 Milan, Italy
29 Institute of Theoretical and Experimental Physics, ITEP, Moscow, Russia
30 INFN-Sezione di Napoli and University of Naples, I-80125 Naples, Italy
31 Department of Natural Sciences, University of Cyprus, Nicosia, Cyprus
32 University of Nijmegen and NIKHEF, NL-6525 ED Nijmegen, The Netherlands
33 Oak Ridge National Laboratory, Oak Ridge, TN 37831, USA
34 California Institute of Technology, Pasadena, CA 91125, USA
35 INFN-Sezione di Perugia and Universitá Degli Studi di Perugia, I-06100 Perugia, Italy
36 Carnegie Mellon University, Pittsburgh, PA 15213, USA
37 Princeton University, Princeton, NJ 08544, USA
38 INFN-Sezione di Roma and University of Rome, "La Sapienza", I-00185 Rome, Italy
39 Nuclear Physics Institute, St. Petersburg, Russia
40 University and INFN, Salerno, I-84100 Salerno, Italy
41 University of California, San Diego, CA 92093, USA
42 Dept. de Fisica de Particulas Elementales, Univ. de Santiago, E-15706 Santiago de Compostela, Spain
43 Bulgarian Academy of Sciences, Central Lab. of Mechatronics and Instrumentation, BU-1113 Sofia, Bulgaria
44 Center for High Energy Physics, Korea Adv. Inst. of Sciences and Technology, 305-701 Taejon, Republic of
    Korea
45 University of Alabama, Tuscaloosa, AL 35486, USA
46 Utrecht University and NIKHEF, NL-3584 CB Utrecht, The Netherlands
47 Purdue University, West Lafayette, IN 47907, USA
48 Paul Scherrer Institut, PSI, CH-5232 Villigen, Switzerland
49 DESY-Institut für Hochenergiephysik, D-15738 Zeuthen, FRG
50 Eidgenössische Technische Hochschule, ETH Zürich, CH-8093 Zürich, Switzerland
51 University of Hamburg, D-22761 Hamburg, FRG
52 High Energy Physics Group, Taiwan, China
§   Supported by the German Bundesministerium für Bildung, Wissenschaft, Forschung und Technologie
‡   Supported by the Hungarian OTKA fund under contract numbers T14459 and T24011.
♭   Supported also by the Comisión Interministerial de Ciencia y Technología
♯   Also supported by CONICET and Universidad Nacional de La Plata, CC 67, 1900 La Plata, Argentina
◇   Also supported by Panjab University, Chandigarh-160014, India
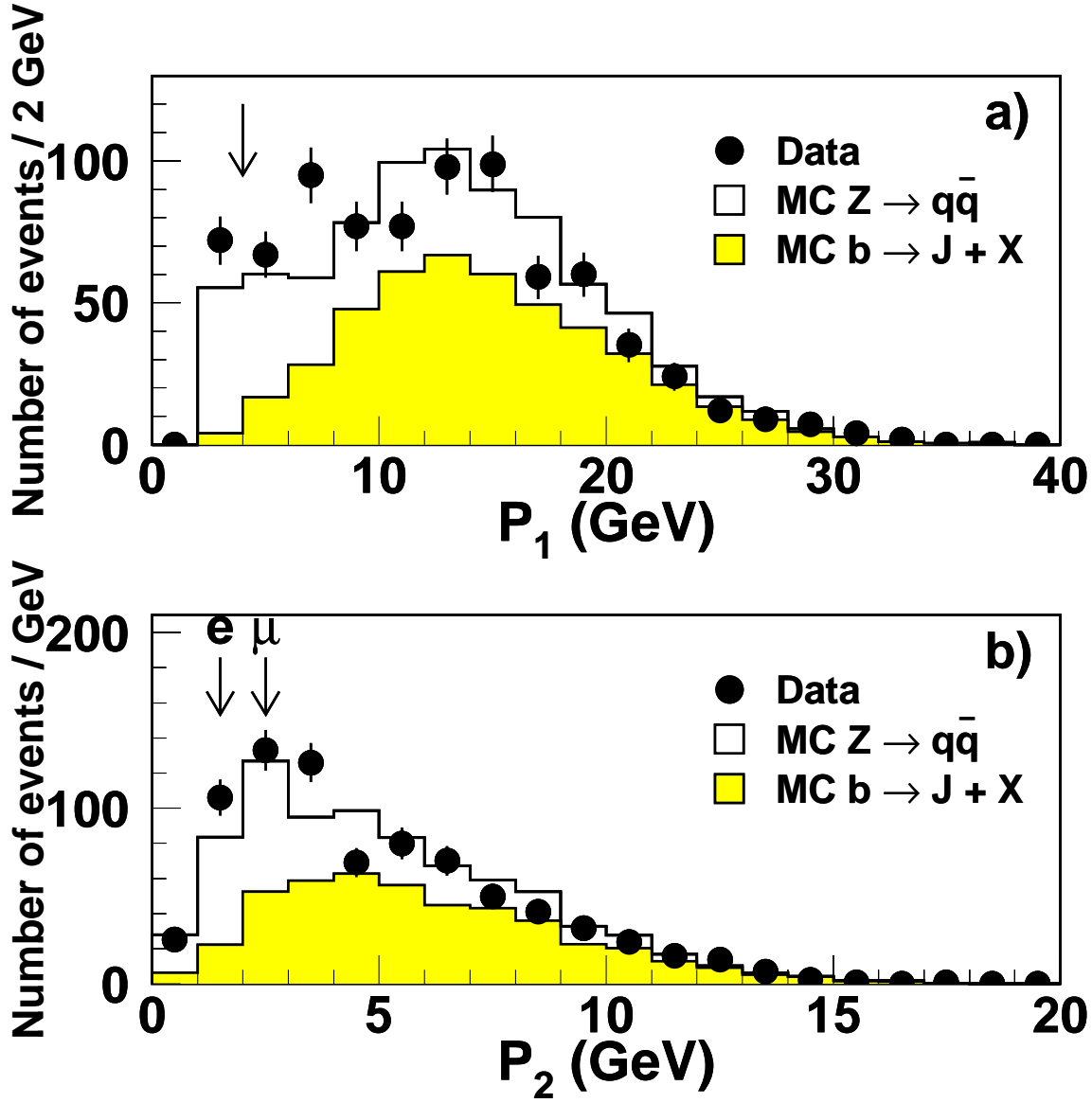△   Supported by the National Natural Science Foundation of China.

Figure 1: Spectrum of (a) the most energetic lepton and (b) the least energetic lepton for $\ell^+\ell^-$ pairs in the mass region $2.8 < M_{\ell^+\ell^-} < 3.4$ GeV. All selection cuts are applied but the ones on the lepton momenta. The arrows indicate the position of the cuts.
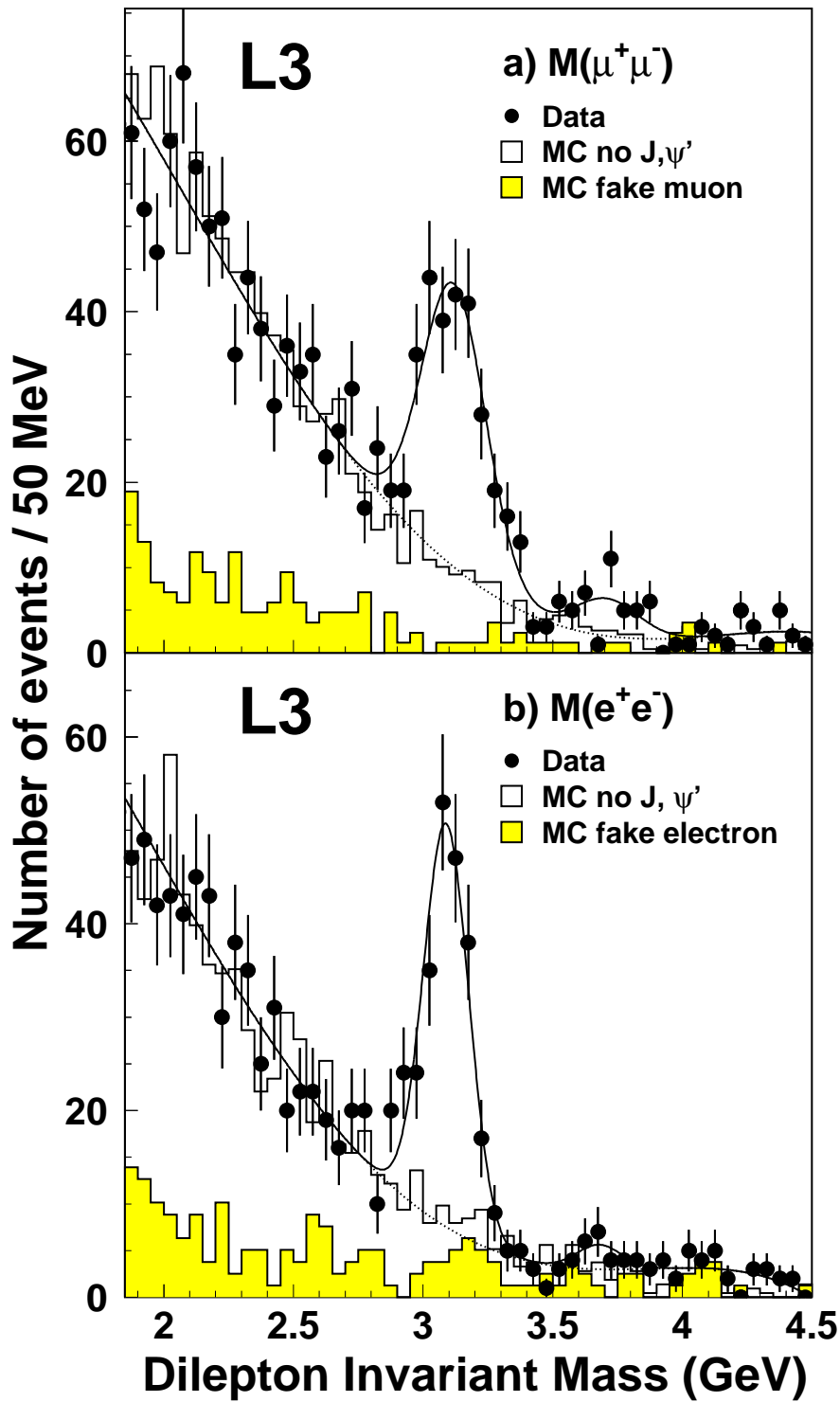
Figure 2: (a) Invariant mass spectrum of $\mu^+\mu^-$ and (b) e^+e^- selected pairs. The line represents the result of the unbinned maximum-likelihood fit described in the text.
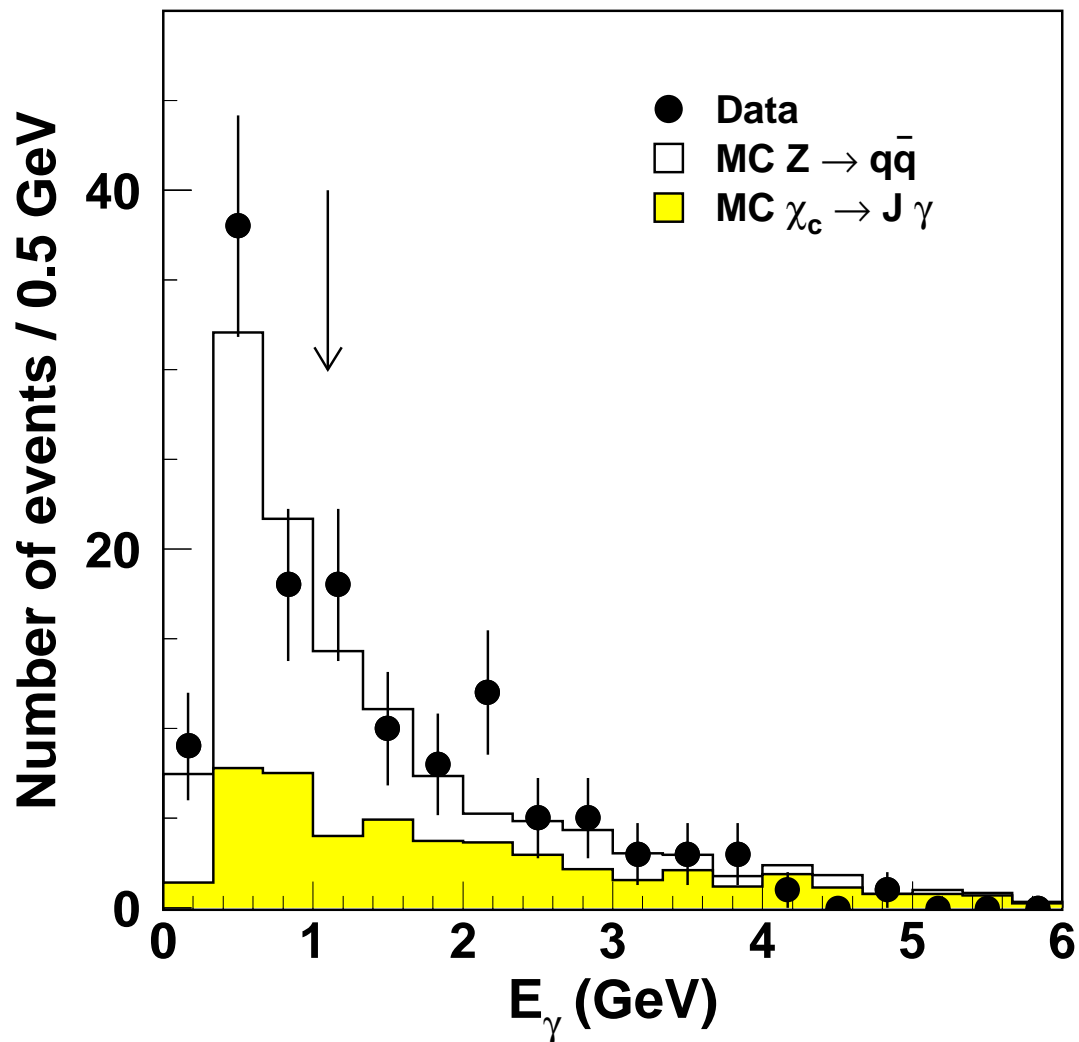
Figure 3: Spectrum of photons in the mass region $M(\ell^+\ell^-\gamma) - M(\ell^+\ell^-) = (414 \pm 56)$ MeV, after all selection cuts are applied but the one on the photon energy. The arrow indicates the position of the cut.
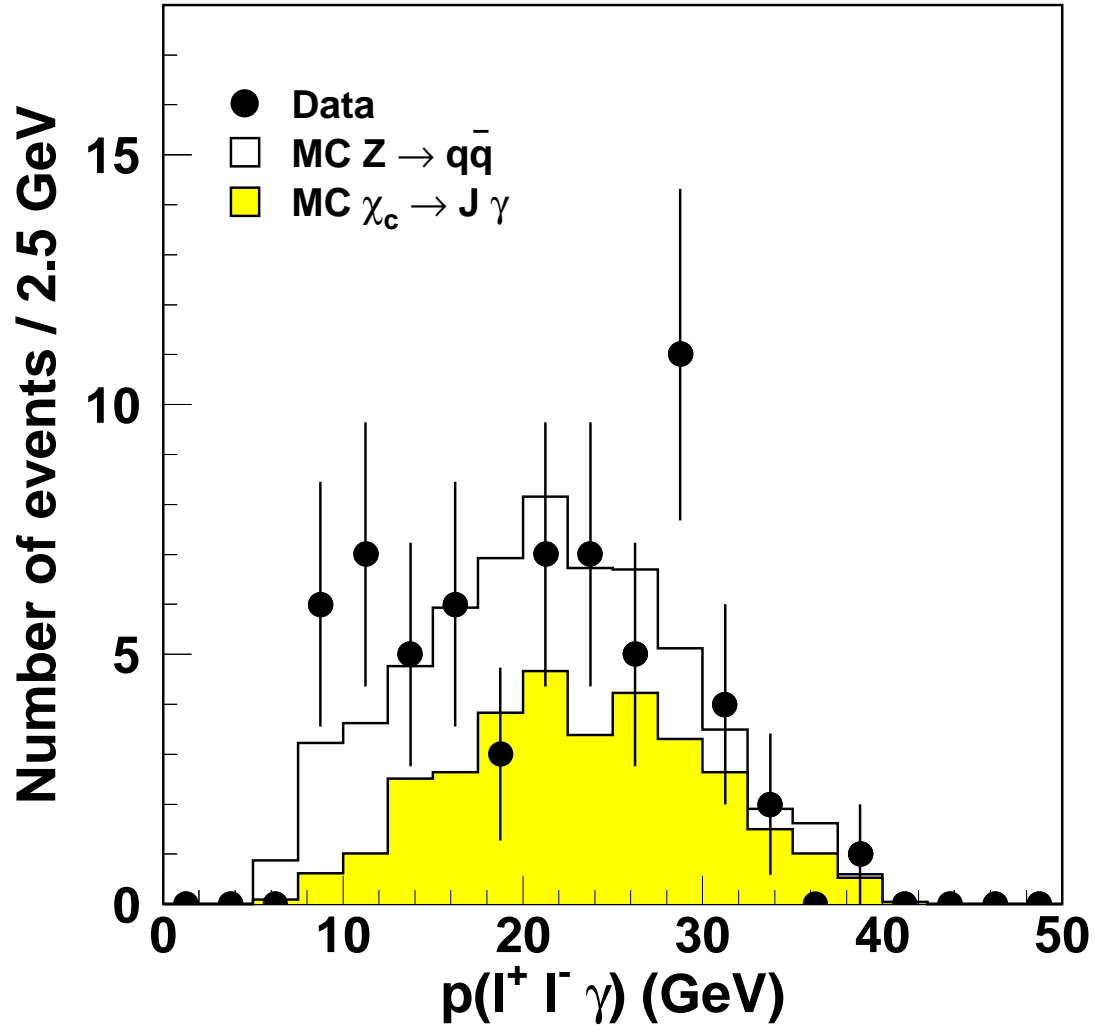
Figure 4: Momentum of $\ell^+\ell^-\gamma$ combinations in the $M(\ell^+\ell^-\gamma) - M(\ell^+\ell^-) = (414 \pm 56)$ MeV mass region.
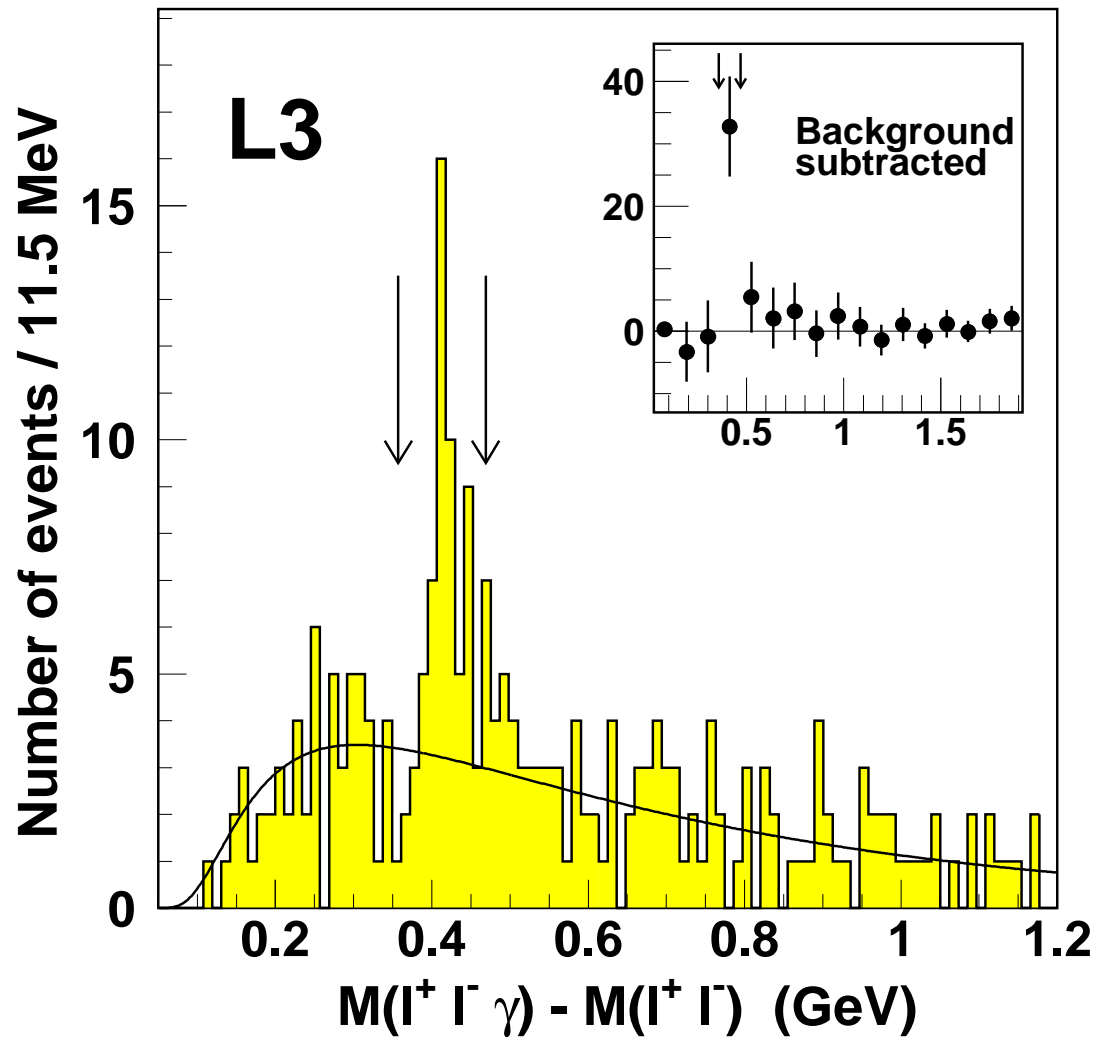
Figure 5: Measured $M(\ell^+\ell^-\gamma) - M(\ell^+\ell^-)$ spectrum. The arrows delimit the signal region. In the insert the background subtracted distribution is shown.
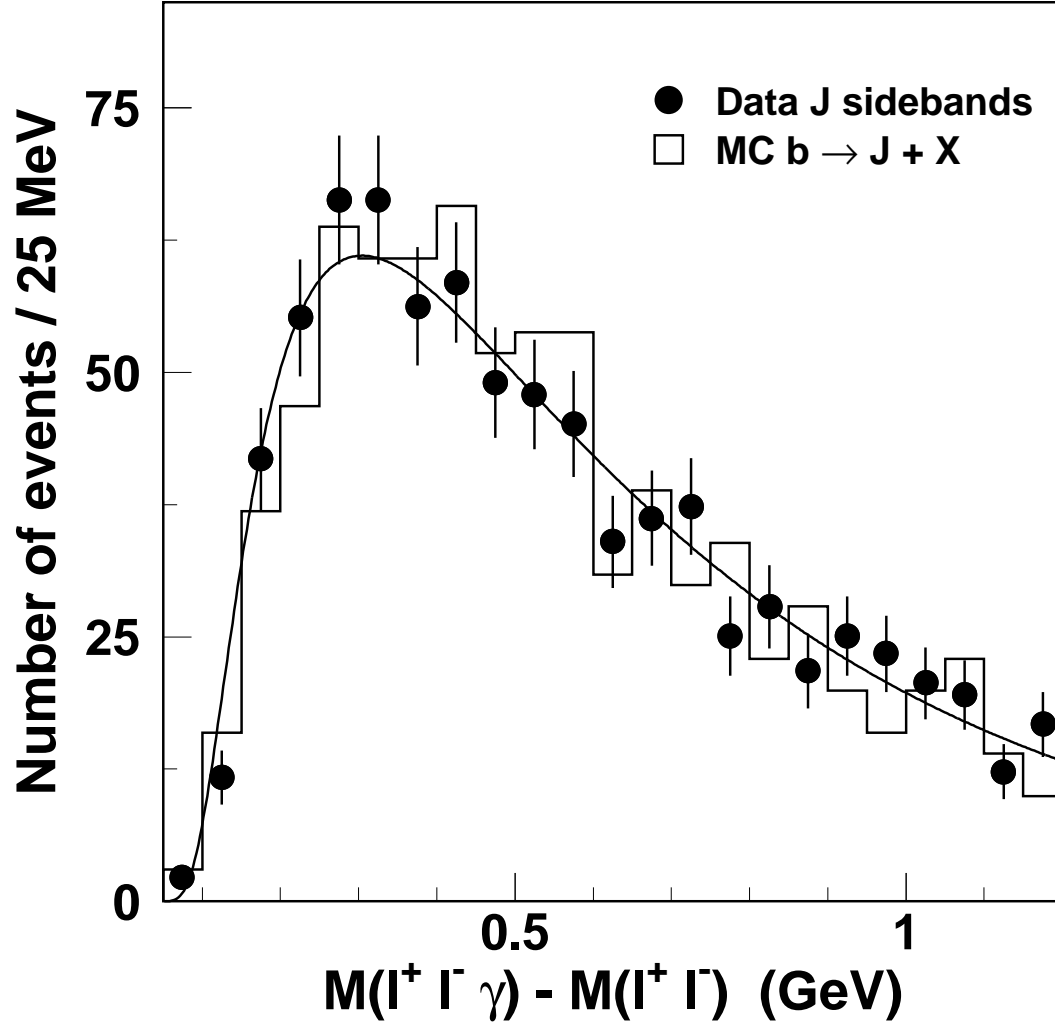
Figure 6: $M(\ell^+\ell^-\gamma) - M(\ell^+\ell^-)$ background. The points are data taken from the sideband of the J peak and from $e^{\pm}\mu^{\mp}$ pairs in the J mass region (fake J background) associated with inclusive photon candidates. The histogram is the prediction from the Monte Carlo of inclusive J production without χ_c states (background due to random $J - \gamma$ combinations). The curve is the background shape fitted from the sum of the two types of background. The normalisation is to the expected fake J background.
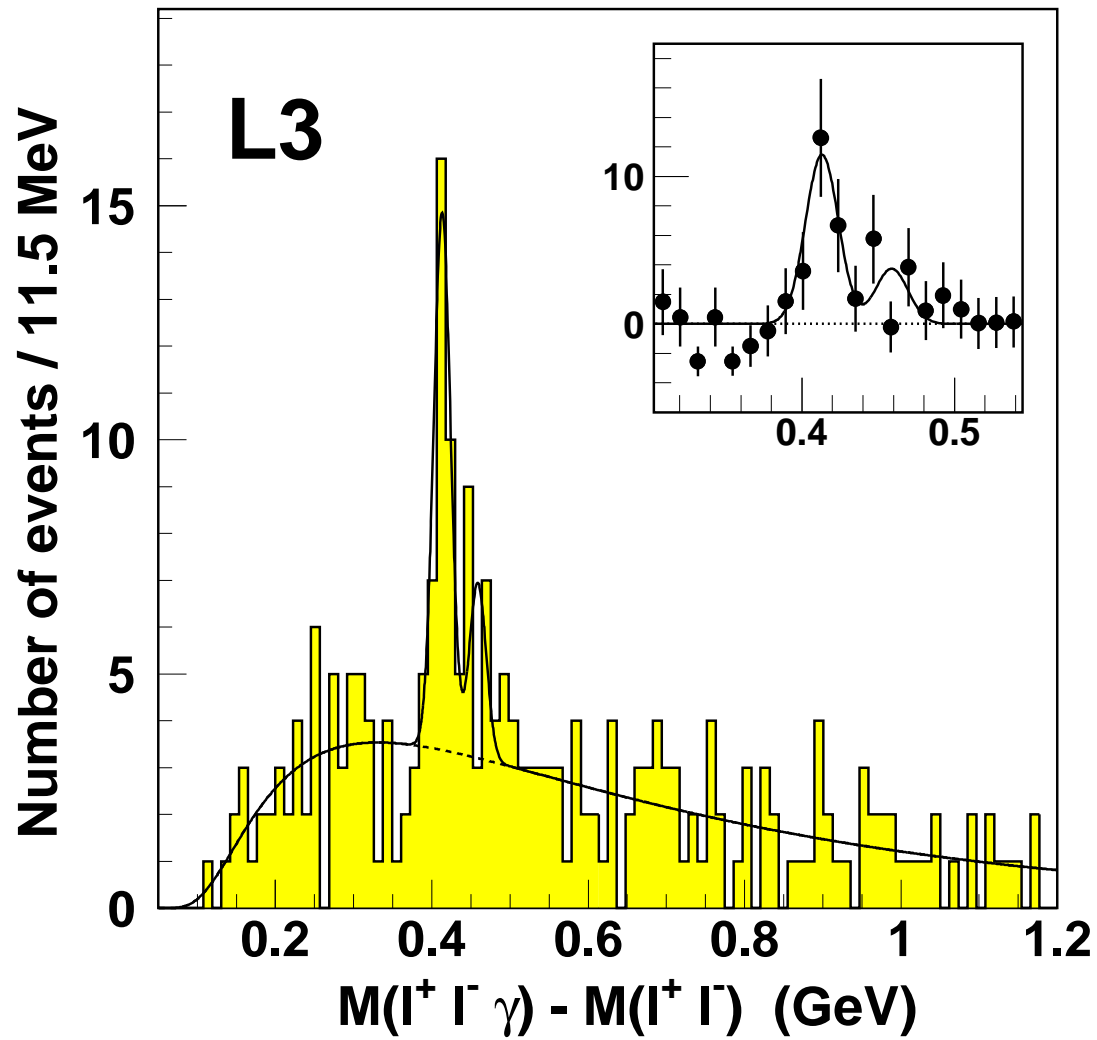
Figure 7: Maximum likelihood fit to the $M(\ell^+\ell^-\gamma) - M(\ell^+\ell^-)$ mass difference spectrum. In the insert the background-subtracted distribution of the signal region is shown.